Synthesis of Mullite Fibre from an Aluminosiloxane Precursor

Toshinobu Yogo*[a] and Ilhan A. Aksay[b]
[a] *Department of Applied Chemistry, School of Engineering, Nagoya University, Furo-cho, Chikusa-ku, Nagoya 464-01, Japan*
[b] *Princeton Materials Institute, Princeton University, Princeton, New Jersey 08544-5263, USA*

Mullite fibre was successfully synthesized by pyrolysis of aluminosiloxane formed from ethyl 3-oxobutanoatodiisopropoxyaluminium and di-(sec-butoxy)aluminoxytriethoxysilane. Aluminosiloxane increased in viscosity with increasing coordination number of aluminium, which was analysed by ^{27}Al NMR spectroscopy. The viscosity of aluminosiloxane was controlled by the amount of added glacial acetic acid as well as the working temperature for the spinning of precursor fibre. Aluminosiloxane gave amorphous SiO_2–Al_2O_3 at 500 °C, which began to crystallize to mullite at 930 °C. Single-phase mullite was produced on heating to 1000 °C for 1 h. The polymer fibre spun from aluminosiloxane was pyrolysed yielding crack-free mullite fibre at 1000 °C for 1 h.

Mullite ($3Al_2O_3{\cdot}2SiO_2$) has various attractive properties such as high-temperature strength, creep resistance and a low thermal expansion coefficient. Fibre-reinforced materials have been receiving great attention because of their applications in the field of composites materials.[1,2] Alumina, alumina–silica, and alumina–zirconia fibres are mainly used as temperature-resistant fibres.[3] Refractory oxides have extremely high melting points and low viscosity of melts making melt spinning impractical, which leads to the development of chemical techniques including the sol–gel process for the synthesis of ceramic fibres.

The synthesis of silica-stabilized alumina fibres by the sol process using aluminium oxychloride was demonstrated by Morton *et al.*[4] Aluminosilicate and aluminium borosilicate fibres were made *via* similar processes employing aqueous aluminium acetate and colloidal silica.[5] Horikiri *et al.* reported the fabrication of alumina and silica–alumina fibres from the partially hydrolysed diethylaluminium isopropoxide and polysilicic acid esters.[6]

Usually, the spinning conditions are critical in the sol–gel process, since the viscosity of the sol changes with time, and increases very rapidly once gelation starts. The control of viscosity during rapid gelation, therefore, is a key processing factor, since the viscosity of the sol is not sufficiently high for spinning. Soluble organic polymers, such as polyvinyl alcohol and polyethylene oxide, were added not only to raise the viscosity of the sols but also to improve their spinning characteristics.[4] On the other hand, the time-independent viscosity of the starting polymer in the polymer route is one of the most distinct differences from the sol–gel process. Various spinning methods, such as melt-spinning and dry-spinning result from the suitable solubility and viscoelastic properties of polymers.

Andrianov synthesized various metalloxane polymers including aluminosiloxanes, which comprise Al—O—Si backbones.[7] Organoaluminosiloxane polymer obtained from diacetoxydimethylsilane and ethyl acetoacetatealuminium diisopropoxide was used for the fabrication of aluminosilicate films on metal substrates.[8,9] Oxyalkoxide polymer synthesized from aluminium butoxide and tetrachlorosilane was reported to form mullite when the initial Al : Si ratio was appropriate.[10]

The formation process of mullite in the solution–precipitation processes in aqueous systems depends upon the mixing level of aluminium and silicon in the precipitated powders.[11] The difference of the hydrolysis rates between aluminium alkoxide and silicon alkoxide results in the segregation of aluminium- and silicon-containing species in the precipitated powders.[11] The degree of formation of silica and Al–Si spinel during mullitization is explained by the segregation level of starting materials.[12] The slow hydrolysis/condensation of alkoxides under controlled conditions[12–14] and the spray pyrolysis of aluminium nitrate–silicon ethoxide system[15] are reported to be effective for chemical homogeneity in the powders. When the formation of mullite is accompanied by Al–Si spinel and silicious phase, the mechanical properties of the mullite degrade at high temperatures due to the formation of a grain-boundary liquid phase.[15] The synthesis of single-phase mullite is required to achieve the optimal high-temperature properties.

This paper describes the synthesis of mullite fibre from an aluminosiloxane precursor synthesized by the reaction of ethyl 3-oxobutanoatodiisopropoxyaluminium and di-(*sec*-butoxy) aluminoxytriethoxysilane in the presence of glacial acetic acid. The synthesis conditions using glacial acetic acid were found to be useful for avoiding the segregation of aluminium- and silicon-containing species as well as avoiding gelation of the precursor. Aluminosiloxane with controlled viscosity was spun into precursor fibres, which were successfully crystallized in crack-free, single-phase mullite fibres.

Experimental

Starting Materials

Ethyl 3-oxobutanoatodiisopropoxyaluminium, (*iso*-$C_3H_7O)_2Al(CH_3COCHCO_2C_2H_5)$, (EOPA) was prepared according to Patterson *et al.*[16] Di-(*sec*-butoxy)aluminoxytriethoxysilane, (*sec*-$C_4H_9O)_2Al{-}O{-}Si(OC_2H_5)_3$, (BAES) was commercially available (Hüls America Inc., Piscataway, NJ, USA). Glacial acetic acid was refluxed over diphosphorus pentaoxide, and distilled before use.

Synthesis of Mullite Precursor

The synthesis of an aluminosiloxane precursor with a mullite composition ($3Al_2O_3{\cdot}2SiO_2$, Al : Si = 3) was carried out under an argon atmosphere without any solvent.

A mixture of EOPA (18.37 g, 66.61 mmol) and BAES (11.74 g, 33.30 mmol) with an Al : Si ratio of 3 was refluxed at 220 °C for 2 h. After cooling to room temperature, glacial acetic acid (3.20 g, 53.29 mmol, 80 mol% of EOPA) was added dropwise to the reaction mixture to give an exothermic reaction. The resulting viscous liquid was refluxed at 200 °C for 4 h. After the reaction mixture was cooled to room temperature, the low boiling components (< 85 °C/10^5 Pa) were distilled out from the reaction mixture affording a viscous liquid as a residue. The volatile components were removed

thoroughly from the residue at 50 °C and 10^2 Pa for 5 h providing a transparent pale-yellow liquid with an extremely high viscosity.

Synthesis of Powder

The viscous metallo-organic product was heated from room temperature to 500 °C at 1 °C min^{-1} in air using a muffle furnace with a 6000 cm^3 chamber. The powder thus formed was heat-treated at temperatures between 900 and 1200 °C.

Synthesis of Mullite Fibre

The precursor was charged in a brass extruder (Fig. 1), which was then set in a hand press (Riken Seiki, P-16B). The precursor was melted in the extruder using a flexible heater above 80 °C, and then extruded through the spinneret with a diameter of 300 μm below 60 °C. The temperature was measured using a calibrated thermocouple set inside the heater. The extruded fibre was collected with a glass rod. The fibre diameter ranged from 100 to 200 μm. Alternatively, precursor fibres were spun from a bulk polymer with hand-drawing using a glass rod of diameter of 8 mm at room temperature. The length of fibre was 50–80 cm. The polymer fibres were dried in air at room temperature for 2 or 3 days prior to heat treatment. The diameter of fibre by hand-drawing was 5–100 μm. The polymer fibres were cut into lengths of 3–6 cm, and then fired in air from room temperature to 900 °C at 0.2 °C min^{-1}. The ceramic fibres were subsequently heat-treated between 1000 and 1200 °C for 1 h at 1 °C min^{-1} above 900 °C.

Characterization of Aluminosiloxane and Aluminosilicate

Aluminosiloxane and organic products were characterized by IR (Hitachi, 260–30), NMR spectroscopy and gas chromatography (GC, Hitachi, 263–50). IR spectra of organic and metallo-organic products were measured by the liquid-film method using a pair of KBr plates (4 mm thick and 30 mm diameter). The powder samples were mixed with KBr powders and pressed to disks (0.3 mm thick and 10 mm diameter), and then measured. ^{13}C NMR spectra were recorded by a Gemini 200 spectrometer (Varian) in $CDCl_3$ solution using tetramethylsilane as an internal standard. Solution ^{27}Al NMR spectra were measured using a Bruker AC 250 spectrometer at 65.18 MHz in $CDCl_3$ solution with $Al(H_2O)_6^{3+}$ as an external standard. The volatile components as reaction by-products were collected by a chilled trap immersed in a dry-ice–acetone bath, and analysed by ^{13}C NMR and GC. The viscosity of precursor was measured by a rotational viscometer using a cone-and-plate (Tokyo Keiki, EHD) from 45 to 75 °C. Molecular weights were determined cryoscopically using benzene as a solvent.[17]

The crystallization behaviour of the amorphous product was measured with DTA and TG (Perkin-Elmer, 7) at a heating rate of 10 °C min^{-1}. The pyrolysis product was analysed by X-ray diffraction analysis (XRD) with Cu-Kα radiation (Rigaku, RAD-II) after heat treatment at temperatures between 900 and 1200 °C from 1 to 10 h. Ceramic fibres were observed by scanning electron microscopy (SEM) using a JEOL JSM-T20. The ratio of aluminium to silicon in the mullite fibres was analysed by ICP (inductively coupled plasma) emission spectroscopy (Shimadzu ICPQ-1000). The solution for ICP analysis was prepared according to the literature.[18] The density of fibres was determined by a sink-float method using a mixture solution of thallium formate and thallium malonate.

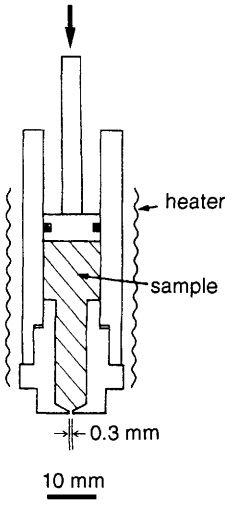

Fig. 1 Extrusion apparatus of aluminosiloxane precursors

Results and Discussion

Synthesis of Aluminosiloxane for Mullite

A mixture of EOPA and BAES with a molar ratio of 2 (the Al:Si atomic ratio of 3) was reacted with various amounts of glacial acetic acid yielding viscous liquids. The product was transparent, and soluble in usual organic solvents, such as benzene and chloroform. No water was used for the reaction in order to avoid the gelation of products.

BAES has an advantage for molecular mixing of aluminium and silicon, since it has an Al—O—Si bond in monomer itself. In addition, the silicon site of BAES is at least trifunctional to condensation reaction because three ethoxy groups are bonded to the silicon atom. The multifunctional silicon compound has higher possibility for the formation of cross-linkage and branching *via* M—O bonds than that of di- and monofunctional compounds. Since silicon-organics consisting of Si—OR (R = methyl, ethyl) bonds are generally less volatile than those including Si—R bonds, the loss of silicon moieties can be minimized during calcination. Also, EOPA is a difunctional compound, since the isopropyl group is more susceptible than the chelate ligand for the elimination and substitution reaction. The M—O—M′ (M,M′ = Al and Si) bond in a starting aluminosiloxane is introduced to minimize the loss of silicon and aluminium moiety during the initial stage of pyrolysis below 300 °C.

Characterization of Aluminosiloxane for Mullite

IR spectra of starting EOPA–BAES mixture of mullite composition ($3Al_2O_3 \cdot 2SiO_2$, Al:Si = 3, a molar ratio of EOPA:BAES = 2) and its reaction product with 8.0 mol% acetic acid are shown in Fig. 2. The spectrum of starting mixture shows the absorption bands ascribed to Al—O bond at 570, 630 and 700 cm^{-1} [Fig. 2(*a*)].[19] The bands changed from sharp peaks to a broad coalesced band after the treatment of acetic acid as shown in Fig. 2(*b*). This change suggests the formation of a product with various kinds of Al—O bond including ligand-exchange reactions. The Si—O absorption bands of Al—O—Si bond are reported to appear at 1064 and 810 cm^{-1}.[19] BAES itself shows the absorption at 1060 cm^{-1} as well as those of Si—O at 770 and 670 cm^{-1}. However, these bands are covered with those of EOPA in Fig. 2. The reaction product between BAES and 8 mol% AcOH shows the decrease in intensity and broadening of these absorptions at 1060, 770 and 670 cm^{-1}. The Al—O—Si bond in the

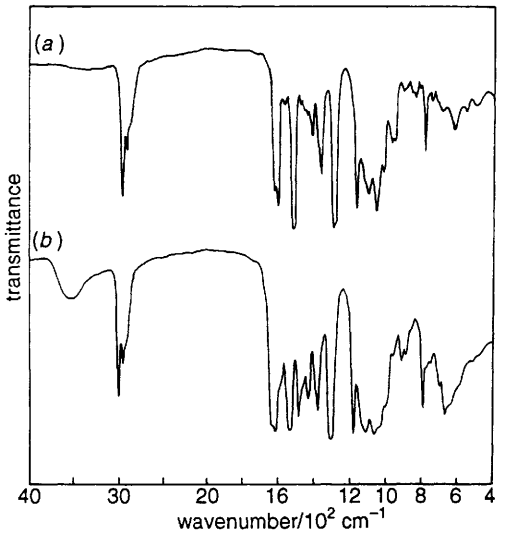

Fig. 2 Infrared spectra of starting EOPA–BAES(2:1) and polymeric product: (*a*) starting EOPA–BAES (2:1); (*b*) polymeric product formed from EOPA–BAES–8 mol% acetic acid

EOPA–BAES mixture may, therefore, undergo the ligand redistribution including the cleavage of the Al—O—Si bond. Both 2(*a*) and 2(*b*) contained the absorption bands due to ethyl 3-oxobutanoato ($CH_3COCHCO_2C_2H_5$, EOB) ligand at 1640, 1620, 1535 and 1300 cm^{-1}. The OH absorption at 3500 cm^{-1} in Fig. 2(*b*) shows the formation of a small amount of water or alcohols in the reaction product.

Fig. 3 shows the change of ^{13}C NMR spectra of EOPA–BAES (molar ratio, 2) with the amount of acetic acid. The signals of the starting mixture of EOPA and BAES in

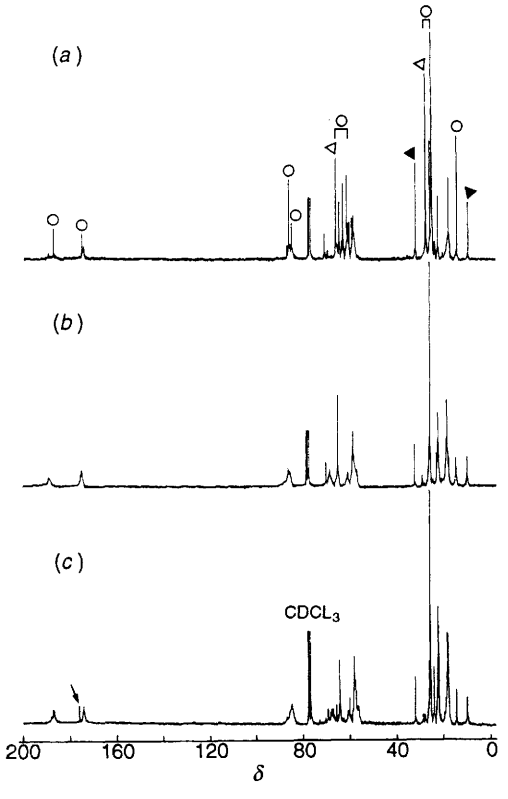

Fig. 3 ^{13}C NMR spectra of starting EOPA–BAES(2:1) and polymeric products synthesized from EOPA–BAES and various amounts of acetic acid: (*a*) starting EOPA–BAES; (*b*) product formed from EOPA–BAES and 8 mol% AcOH; (*c*) product formed from EOPA–BAES and 30 mol% AcOH

Fig. 3(*a*)† were assigned according to the literature.[20] The main signals of free ethyl 3-oxobutanoate (EOB) appear at 50.3, 167.6 and 201.3 ppm. These signals shifted to 86.0, 174.9 and 187.2 ppm, respectively, due to coordination to aluminium [Fig. 3(*a*)]. The signals of EOPA are marked with ○ in Fig. 3(*a*). The others are assigned to BAES. The sharp signals of EOB in the starting EOPA–BAES changed to broad multiplet on treatment with acetic acid as shown in Fig. 3(*b*). The multiplet results from carbons having slightly different chemical environment from each other. The signals assigned to isopropoxy (27.9 and 66.0 ppm, marked with ▽) and *sec*-butoxy groups (10.0 and 32.0 ppm, marked with ▼) decreased in intensity with increasing amount of acetic acid as shown in Fig. 3(*b*) and 3(*c*). The alkoxy groups on aluminium atoms in both EOPA and BAES are eliminated on treating with acetic acid. However, the alkoxy groups still remain in the product treated with 30 mol% of acetic acid, since the signals of alkoxy groups are observed in Fig. 3(*c*).

The elimination of both the isopropoxy from EOPA and the *sec*-butoxy group from BAES shows the possibility of the cross-condensation reaction between EOPA and BAES. The new signal at 176.2 ppm with an arrow in Fig. 3(*c*) appeared with increasing amount of acetic acid from 8 to 30 mol%. The signal is assigned to the carboxy carbon of CH_3CO_2 group substituted on metals, since free acetic acid shows a signal at 178.7 ppm. The signal at 176.2 ppm was not observed for the reaction product from EOPA itself and 30 mol% acetic acid. Therefore, the substitution of alkoxy groups on silicon for the carboxy group of acetic acid proceeds yielding the signal at 176.2 ppm. Glacial acetic acid not only eliminates the alkoxy groups from EOPA–BAES but also substitutes alkoxy groups for CH_3CO_2 at the concentration of 30 mol% acetic acid.

Fig. 4 shows solution ^{27}Al NMR spectra of starting EOPA–BAES and its reaction products with acetic acid. The starting EOPA–BAES has a signal at 4.2 ppm, and broad signals centred at 40 and 62 ppm. The broad signal centred at 62 ppm derives from four-coordinated aluminium.[21,22] The signal at 40 ppm is assigned to five-coordinated aluminium.[22,23] A monomeric EOPA is four-coordinated, since EOB is a bidentate ligand including two carbonyl oxygens coordinating aluminium. The strong resonance at 4.2 ppm is due to the six-fold coordination of aluminium–oxygen octahedra.[21] On the basis of these results, EOPA or BAES associates affording dimers in $CDCl_3$ solution as reported on aluminium alkoxides, such as $Al(OC_2H_5)_3$, $Al(O^iC_3H_7)_3$ and $Al(O^iC_4H_9)_3$.[22]

The signal at 4.2 ppm in the starting EOPA–BAES increased in half-value width by the reaction with acetic acid from Fig. 4(*a*) to 4(*b*). The half-value width of the signals at 4.2 ppm in Fig. 4(*a*), 4(*b*) and 4(*c*) are 391, 769 and 965 Hz, respectively. ^{27}Al ($I=5/2$) is one of the quadrupole nuclei. The linewidth of a quadrupole nucleus is strongly related to its quadrupole moment and the value of the electric-field gradient along the

†EOPA, isopropoxy $^1CH_3{}^2CHCH_3$, ^1C 27.7, 27.9, ^2C 66.0, 66.8 ppm.

EOB $^3CH_3{}^4C{}^5CH{}^6CO{}^7CH_2{}^8CH_3$, ^3C 25.2, 26.0, ^4C 187.2, ^5C 86.0, 84.7, ^6C 174.9, ^7C 61.3, 62.8, ^8C 14.5, 14.3 ppm.

BAES, *sec*-butoxy $^1CH_3{}^2CH_2{}^3CH{}^4CH_3$, ^1C 10.0, 9.6, ^2C 32.0, 32.2, ^3C 71.4, 64.6, ^4C 22.7, 25.0 ppm.

ethoxy $O^5CH_2{}^6CH_3$, ^5C 58.3, ^6C 18.1 ppm.

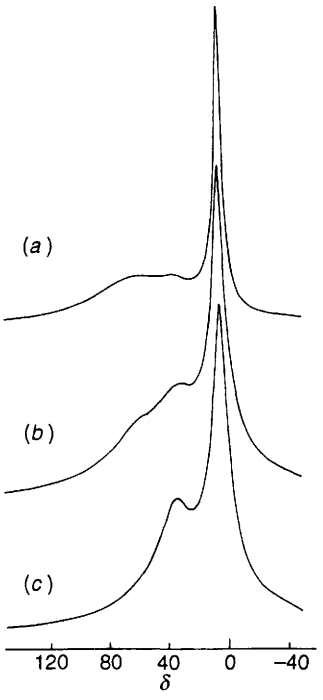

Fig. 4 Change of ^{27}Al NMR spectra of starting EOPA–BAES(2:1) and polymeric precursor with the amount of acetic acid: (*a*) starting EOPA–BAES; (*b*) product formed from EOPA–BAES and 8 mol% AcOH; (*c*) product formed from EOPA–BAES and 80 mol% AcOH

bond. A more perfect cubic symmetry (O_h or T_d) arrangement of substituent about ^{27}Al decreases the electric-field gradient yielding sharper lines.[21] Thus, the broadening of the signal is attributable to the increase both in distortion and imbalance around octahedrally coordinated aluminium.[21] This change shows the redistribution of ligands around aluminium through the reaction of aluminium compounds to each other as well as with acetic acid. The signal at 35 ppm increased in intensity after treatment with 8 mol% acetic acid as shown in Fig. 4(*b*). When EOPA–BAES was allowed to react with 80 mol% acetic acid, the signal at 35 ppm continued to increase, and the four-coordinated aluminium at 62 ppm almost disappeared in the broad signal centred at 35 ppm as shown in Fig. 4(*c*). EOPA–BAES reacts with acetic acid as a chelating ligand increasing the amount of higher coordinated aluminium atom, which is sterically more crowded aluminium than that of starting EOPA–BAES.

The molecular weight of the EOPA–BAES mixture was 550±30 [calcd. for EOPA–BAES(2:1), 282.4] with cryoscopic measurements in benzene. This indicates that the starting EOPA or BAES associates affording an equilibrium mixture. The molecular weight of polymeric product increased from 590±30 to 1050±50 when the molar percent of acetic acid was raised from 2.5 to 30 mol%. Therefore, the product consists mainly of dimers and trimers.

The reaction between EOPA–BAES and acetic acid gave a mixture of aluminosiloxane and low boiling point components. The low boiling point products comprise alkyl alcohol and its acetate. The formation of ethyl, isopropyl and *sec*-butyl alcohol and corresponding ethyl, isopropyl and *sec*-butyl acetate was confirmed by ^{13}C NMR and GC. The amount of alkoxy groups obtained as these alcohols and acetates ranged from 25 to 35% of the total amounts of alkoxy groups in the starting EOPA–BAES. Glacial acetic acid eliminates alkoxy groups from EOPA–BAES by a substitution reaction:

$$M(OR)_n + CH_3CO_2H \rightarrow M(OR)_{n-1}(OCOCH_3) + ROH \quad (1)$$

Also the eliminated alkoxy groups reacted with acetic acid yielding water and acetates:

$$ROH + CH_3CO_2H \rightarrow CH_3CO_2R + H_2O \quad (2)$$

Acetate species may again undergo transesterification with metal alkoxides in the reaction mixture.[24]

$$M(OR)_n + xCH_3CO_2M' \rightarrow M(OR)_{n-x}(OM')_x + xCH_3CO_2R \quad (3)$$

M—O—M′ bonds could be formed according to the transesterification as well as according to the usual condensation between M—OH and M′—OR, since a small amount of water was formed in the reaction system. The limited amount of water generated by the reaction between acetic acid and eliminated alcohol suppresses the further condensation, resulting in the formation of the oligomeric precursors. The reaction between EOPA–BAES and acetic acid is summarized as follows, although the formation process of the mullite precursor is composed of several reactions:

$$(Pr^iO)_2Al(EOB) + (Bu^sO)_2Al{-}O{-}Si(OEt)_3 \xrightarrow{CH_3CO_2H} RO\left(-\underset{\displaystyle L^1}{\overset{}{\underset{|}{}}}Al-O-\underset{\displaystyle L^2}{\overset{}{\underset{|}{}}}Si-\underset{\displaystyle L^3}{\overset{}{\underset{|}{}}}\right)_n + ROH + CH_3CO_2R + H_2O \quad (4)$$

L^1 = EOB, L^2, L^3 = OEt, OR, OAc, OM

The polymeric product has ethyl 3-oxobutanoato (EOB) ligands on the basis of IR and ^{13}C NMR spectroscopy (Fig. 2 and 3). The oligomers in the polymeric product consist of a structure unit of [-Al(EOB)-O-], which undergoes the intermolecular association affording an octahedrally coordinated aluminium. Since alkoxy groups remain bonded to aluminosiloxane as shown in Fig. 3(*c*), a structure of -Al(EOB)(OR)-O- might constitute a part of five-coordinated aluminiums.

Viscosity and Spinnability of Polymeric Precursor

The change of viscosity at 75 °C with the amount of added acetic acid is shown in Fig. 5. Both EOPA and BAES are

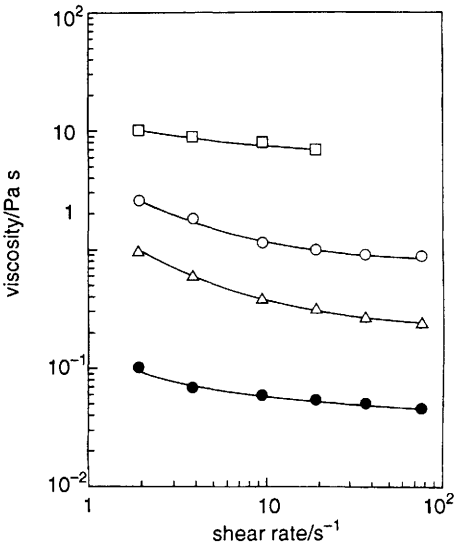

Fig. 5 Change of viscosity for polymeric precursor with the amount of acetic acid and shear rate at 75 °C: ●, starting EOPA–BAES; △, EOPA–BAES–2.5 mol% AcOH; ○, EOPA–BAES–30 mol% AcOH; □, EOPA–BAES–50 mol% AcOH

liquids at room temperature. However, the magnitude of viscosity below 0.1 Pa s for the starting EOPA–BAES was not high enough for spinning. The viscosity increased by one order of magnitude on treatment with only 2.5 mol% acetic acid, and then continued to increase with increasing amounts of acetic acid from 30 to 50 mol%. The increase in molecular weight is responsible for the increase in viscosity. Also, the viscosity of product increases by the intra- and inter-molecular coordination of aluminium, which increases the coordination number of oxygen to aluminium atom as shown in Fig. 4.

Fig. 6 shows the relation between viscosity and $1/T$ for the starting EOPA–BAES and EOPA–BAES–AcOH at a constant shear rate of 1.9 s^{-1}. The logarithm of viscosity has a linear relationship to the temperature, and follows the Andrade (Arrhenius) equation. The activation energies calculated from the $\log \eta$–$1/T$ slopes are 10.5 (no AcOH), 91.0 (30 mol% AcOH) and 132.0 kJ mol^{-1} (50 mol% AcOH), and increase with increasing amount of acetic acid. The increased activation energy for flow reflects the increase in the chain length and in the interchain interactions of the polymer.[25]

The product formed from EOPA–BAES and glacial acetic acid had a time-independent and stable viscosity. The precursor viscosity can be controlled by the amount of AcOH and the working temperature. The viscosity for EOPA–BAES–30 mol% AcOH decreased in magnitude from 50.2 Pa s (502 poise) to 2.76 Pa s (27.6 poise) on increasing the measurement temperature from 45 to 75 °C. The precursor formed from EOPA–BAES–30 mol% AcOH was extruded through a spinneret into a fibrous shape. The viscosity of the present precursor suitable for extrusion was found to be from several Pa s to 10^2 Pa s in Fig. 6. The working temperature for extrusion was from 30 to 50 °C. The shear thinning behaviour of the precursor enables spinning. Cooling after the extrusion results in the increased viscosity, which also favours spinning.

On the other hand, the viscosity for hand-drawing was *ca.* 10^2 Pa s^{-1}. The viscosity range for hand-drawing was smaller than that for extrusion.

The dry-spinning of the precursor also results from the complete solubility of the aluminosiloxane in organic solvents. The precursor fibre was drawn from the benzene solution of precursor with the concentration above 80 wt.% at room temperature using a glass rod. The fibre diameter ranged from 10 to 200 μm.

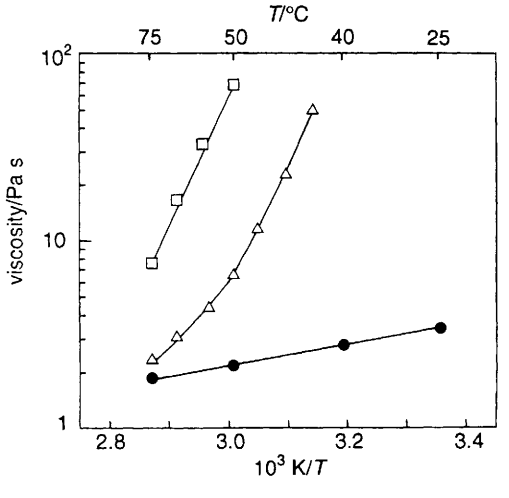

Fig. 6 Variation of viscosity for precursor formed from EOPA–BAES–AcOH with measurement temperatures at a shear rate of 1.9 s^{-1}: ●, starting EOPA–BAES; △, EOPA–BAES–30 mol% AcOH; □, EOPA–BAES–50 mol% AcOH

Synthesis of Mullite from Aluminosiloxane Precursor

The aluminosiloxane formed from EOPA–BAES–50 mol% AcOH was heated from room temperature to 500 °C at 1 °C min^{-1} to afford white powders. The weight loss on heating was *ca.* 73 wt.%.

A halo pattern was observed for the X-ray diffraction of the product formed at 500 °C. The IR spectrum of the product had a broad absorption centred at 1027 cm^{-1}, which is lower than that of ν(Si–O) for amorphous silica at 1100 cm^{-1}. The shift of the absorption band is attributable to the substitution of Si–O–Si bond for Si–O–Al bond as reported.[26] This fact reflects the formation of $Si(Al)O_4$-tetrahedra in the amorphous silica–alumina.

The DTA and TG curves of the amorphous silica–alumina formed by pyrolysis of EOPA–BAES–50 mol% AcOH at 500 °C are shown in Fig. 7. On heating at 10 °C min^{-1}, the amorphous powder lost the physically absorbed water to give the endothermic peak at 162 °C. The second endothermic peak at 462 °C is due to the loss of water by dehydroxylation reaction. Finally, the amorphous powder crystallized exothermically at 980 °C without weight loss.

Fig. 8 shows the change of XRD patterns of the amorphous silica–alumina powder with heat treatment temperature for 1 h. The amorphous silica–alumina began to crystallize to mullite after heat treatment at 950 °C for 1 h, and then increased its crystallinity on increasing heat-treatment temperature.

The crystallinity of amorphous silica–alumina increased at 930 °C as the duration time increased from 1 to 10 h as shown in Fig. 9. The crystallinity of mullite heat-treated at 930 °C for 10 h [Fig. 9(*c*)] was comparable with that formed at 950 °C for 1 h [Fig. 8(*c*)]. The mullitization of the amorphous powder was found to proceed at 930 °C.

Several papers have reported the crystallization of mullite directly from the amorphous phase.[12–15] Similarly, Al and Si were mixed at the molecular level in the aluminosiloxane of sufficient degree of condensation yielding mullite directly from amorphous silica–alumina.

Synthesis of Mullite Fibre

The viscosity of aluminosiloxane was controlled by the amount of glacial acetic acid for condensation as shown in a previous section. The polymer fibre spun from the aluminosiloxane formed from EOPA–BAES–50 mol% AcOH was burned out to produce ceramic fibres.

The amorphous silica–alumina fibres with mullite composition were formed at 900 °C for 1 h. The amorphous fibres

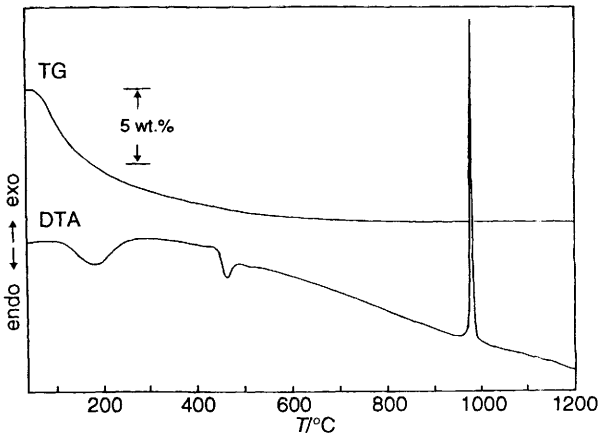

Fig. 7 DTA–TG curves for amorphous silica–alumina formed by pyrolysis of aluminosiloxane at 500 °C

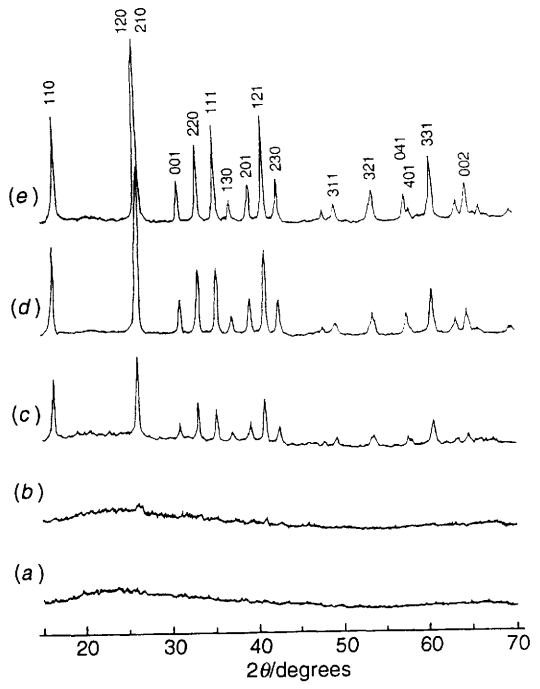

Fig. 8 XRD profiles of pyrolysed products at temperatures from 900 to 1200 °C for 1 h: (*a*) 900 °C; (*b*) 930 °C; (*c*) 950 °C; (*d*) 1000 °C; (*e*) 1200 °C

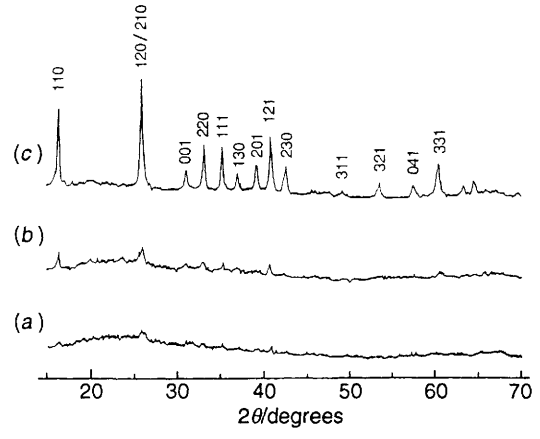

Fig. 9 Change of crystallinity of silica–alumina with duration time at 930 °C: (*a*) 1 h; (*b*) 3 h; (*c*) 10 h

were then heated from 900 to 1200 °C at 1 °C min^{-1} in order to avoid the rapid crystallization shown in Fig. 7. The mullite fibres heat-treated at 1000 °C had smooth surfaces, and diameters from 20 to 100 μm [Fig. 10(*a*)]. The cross-section of fibre was circular, and was composed of quite smooth surfaces as shown in Fig. 10(*b*). The fibres were confirmed to be mullite by XRD analysis. The density of mullite fibres thus formed at 1200 °C was from 3.05 to 3.08 (the reported value of the density for mullite is 3.17 g cm^{-3}).[27] The weight percentage of Al_2O_3 in mullite fibres was found to be 71.2 wt.% (theoretical, 71.80 wt.%) by chemical analysis.

Conclusions

Mullite fibre was synthesized successfully from aluminosiloxane precursor without any additives of polymer for the adjustment of viscosity. The results are summarized as follows. (i) A mixture of ethyl 3-oxobutanoatodiisopropoxyaluminium and di-(*sec*-butoxy)aluminoxytriethoxysilane was reacted with

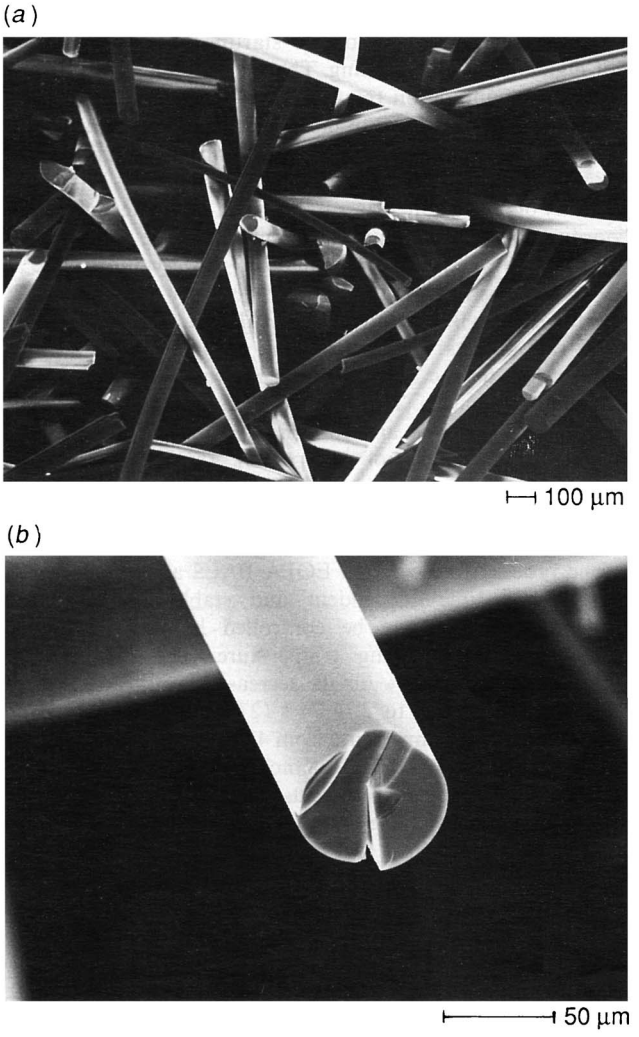

Fig. 10 SEM photographs of mullite fibre synthesized from EOPA–BAES–50 mol% AcOH: (*a*) 1000 °C, 1 h; (*b*) fracture surface of mullite fibre crystallized at 1200 °C for 1 h

glacial acetic acid yielding the viscous precursor for mullite fibre. (ii) The polymeric product had a molecular weight below 1000, and contained the increased amount of five-coordinated aluminium, which is responsible for an appropriate viscosity for spinning. The viscoelastic properties required for the spinning resulted from the oligomeric aluminosiloxane with suitable intra- and inter-molecular coordination. (iii) The viscosity of bulk polymer was independent of time, and was controlled by the selection of temperature in order to obtain the appropriate viscosity for spinning. (iv) The preceramic fibre spun from the polymeric precursor was converted to a single-phase mullite fibre after heat treatment at 1200 °C.

References

1 G. Winter, *Angew. Chem. Intl. Ed. Engl.*, 1972, **11**, 751.
2 G. Geiger, *Am. Ceram. Soc. Bull.*, 1991, **70**, 212.
3 H. G. Sowman, *Am. Ceram. Soc. Bull.*, 1988, **67**, 1911.
4 M. J. Morton, J. D. Birchall and J. D. Cassidy, *Br. Pat.*, 1974, 1 360 199.
5 A. Borer and G. P. Krogseng, *Ger. Offen.*, 1972, 2 210 288.
6 S. Horikiri, K. Tsuji, Y. Abe, A. Fukui and E. Ichiki, *Ger. Offen.*, 1974, 2 408 122.
7 K. A. Andrianov, in *Metalorganic Polymers*, Interscience, New York, 1965, ch. IV.
8 L. V. Interrante and A. G. Williams, *Polym. Prep.*, 1984, **25**, 13.
9 A. G. Williams and L. V. Interrante, in *Better Ceramics through*

Chemistry, ed. C. J. Brinker, D. E. Clark and D. R. Ulrich, Elsevier, Amsterdam, 1984, p. 151.
10 P. D. E. Morgan, in *Better Ceramics through Chemistry II*, ed. C. J. Brinker, D. E. Clark and D. R. Ulrich, Materials Research Society, Pittsburgh, 1986, p. 751.
11 M. D. Sacks, H-W. Lee and J. A. Pask, in *Ceramic Transactions* 6. ed. S. Somiya, R. S. Davis and J. A. Pask, Amer. Ceram. Soc. Inc., Westerville, 1990, p. 167.
12 K. Okada and N. Otsuka, *J. Am. Ceram. Soc.*, 1986, **69**, 652.
13 D. W. Hoffman, R. Roy and S. Komarneni, *J. Am. Ceram. Soc.*, 1984, **67**, 468.
14 J. A. Pask, X. W. Zhang, A. P. Tomsia and B. E. Yoldas, *J. Am. Ceram. Soc.*, 1987, **70**, 704.
15 S. Kanzaki, H. Tabata, T. Kumazawa and S. Ohta, *J. Am. Ceram. Soc.*, 1985, **68**, C6.
16 T. R. Patterson, F. J. Pavlik, A. A. Baldoni and R. J. Frank, *J. Am. Chem. Soc.*, 1959, **81**, 4213.
17 W. L. Jolly, in *The Synthesis and Characterization of Inorganic Compounds*, Prentice-Hall, Englewood Cliffs, N.J., 1970, p. 283.
18 H. Uchida, T. Uchida and C. Iida, *Anal. Chim. Acta*, 1979, **108**, 87.
19 C. G. Barraclough, D. C. Bradley, J. Lewis and I. M. Thomas, *J. Chem. Soc.*, 1961, 2601.
20 E. Breitmaier and W. Voelter, in *Carbon-13 NMR Spectroscopy*, VCH, New York, 1987, pp. 208 and 218.
21 J. W. Akitt, in *Multinuclear NMR*, ed. J. Mason, Plenum Press, New York, 1987, p. 259.
22 O. Kriz, B. Casensky, A. Lycka, J. Fusek and S. Hartmanek, *J. Magn. Reson.*, 1984, **60**, 375.
23 R. Benn, A. Rufinska, H. Lehmkuhl, E. Janssen and C. Kruger, *Angew. Chem. Intl. Ed. Eng.*, 1983, **22**, 779.
24 D. C. Bradley, R. C. Mehrotra and D. P. Gaur, in *Metal Alkoxides*, Academic Press, London, 1978, pp. 33 and 180.
25 L. E. Nielsen, in *Polymer Rheology*, Marcel Dekker, New York, 1977, ch. 3.
26 H. H. W. Moenke, in *The Infrared Spectra of Minerals*, ed. V. C. Farmer, Mineralogical Society, London, 1974, p. 365.
27 JCPDS card, 15-776.

Paper 3/02561F; *Received* 5th *May*, 1993